C. R. Mecanique 346 (2018) 423–431

Contents lists available at ScienceDirect

Comptes Rendus Mecanique

www.sciencedirect.com

"Tepid" Geysers above salt caverns

Geysers tièdes au-dessus des cavités salines

Pierre Bérest [a,*], Benoît Brouard [b], Vassily Zakharov [b]

[a] *Laboratoire de mécanique des solides, École polytechnique, route de Saclay, 91128 Palaiseau cedex, France*
[b] *Brouard Consulting, 101, rue du Temple, 75003 Paris, France*

ARTICLE INFO

Article history:
Received 16 January 2018
Accepted 19 March 2018
Available online 29 March 2018

Keywords:
Geyser
Tepid geyser
Salt cavern
In situ tests in salt caverns
Instability
Outflow test

Mots-clés :
Geyser
Geyser tiède
Cavité saline
Essais en place en cavité saline
Instabilité
Essai de dégorgement

ABSTRACT

The formation of a brine geyser erupting from the wellhead of a large underground salt cavern is described. In most cases, the brine outflow from an opened cavern is slow; it results from the cavern creep closure and the thermal expansion of the cavern brine. These two processes are smooth; however, the brine outflow often is bumpy, as it is modulated by atmospheric pressure variations that generate an elastic increase (or decrease) of both cavern and brine volumes. In addition, when the flow is fast enough, the brine thermodynamic behavior in the wellbore is adiabatic. The cold brine expelled from the cavern wellhead is substituted with warm brine entering the borehole bottom, resulting in a lighter brine column. The brine outflow increases. In some cases, the flow becomes so fast that inertia terms must be taken into account. A geyser forms, coming to an end when the pressure in the cavern has dropped sufficiently. A better picture is obtained when head losses are considered. A closed-form solution can be reached. This proves that two cases must be distinguished, depending on whether the cold brine initially contained in the wellbore is expelled fully or not. It can also be shown that geyser formation is a rare event, as it requires both that the wellbore be narrow and that the cavern be very compressible. This study stemmed from an actual example in which a geyser was observed. However, scarce information is available, making any definite interpretation difficult.

RÉSUMÉ

On décrit un modèle de formation d'un geyser de saumure faisant éruption à la tête de puits d'une caverne créée par dissolution dans une formation saline. Dans la plupart des cas, le débit de saumure sortant d'une caverne ouverte en tête de puits est lent ; il résulte de la convergence de la caverne par fluage du sel et de l'expansion thermique de la saumure contenue dans la caverne. Ces deux effets sont en principe sans à-coup. Cependant, le débit que l'on observe est très irrégulier ; la raison en est qu'il est modulé par les variations de la pression atmosphérique, qui engendrent des variations de volume de la caverne et de la saumure qu'elle contient. De plus, lorsque le débit est suffisamment rapide, le comportement de la saumure dans le puits est adiabatique. La saumure plus froide sortant en tête de puits est remplacée par de la saumure plus chaude entrant par le fond du puits, de sorte que le poids de la colonne s'allège. Le débit augmente alors. Il

* Corresponding author.
E-mail address: berest@lms.polytechnique.fr (P. Bérest).

https://doi.org/10.1016/j.crme.2018.03.004

peut devenir si rapide que les termes d'inertie et de pertes de charge doivent être pris en compte. Un geyser se forme ; il s'arrête lorsque la pression dans la caverne a suffisamment chuté. Une solution explicite est possible ; elle montre que deux cas doivent être distingués, suivant que le contenu initial du puits est complètement expulsé ou non. Elle montre aussi que la formation d'un tel geyser est rare, il faut à la fois que le puits soit étroit et que la caverne soit très compressible. Cette étude a pour origine un geyser réellement observé ; malheureusement, l'information disponible est trop restreinte pour permettre de l'attribuer de façon certaine au mécanisme invoqué.

1. Introduction

Natural geysers form when the water temperature in an underground reservoir is significantly larger than 100 °C and a conduit (typically, vertical fractures) links the reservoir to the ground level. When hot water rises in the conduit, its pressure decreases due to depth change and head losses, until it reaches thermodynamic conditions such that vaporization is possible. The water density decreases, leading to faster flow and, ultimately, a mixture of water vapor and liquid vapor spews at the ground level. "Cold" geysers are generated by underground waters containing a large amount of carbon dioxide. When water rises in a conduit, carbon dioxide partially vaporizes, leading to a decrease in mixture density. In this paper, a different case of a geyser is described. A large (hence, very compressible) salt cavern is linked to the ground level by a cased and cemented wellbore. The wellhead is opened, and a brine outflow is observed. In principle, this flow should be smooth, as it originates in cavern creep closure and brine thermal expansion. However, it is modulated by atmospheric pressure changes, which lead to an elastic change in the cavern's volume. In addition, when the outflow is fast enough, the brine evolution in the wellbore is adiabatic, and the wellbore brine is substituted with warmer and lighter brine from the cavern, leading to a decrease in brine column weight, still faster flow and, ultimately, the formation of a brine geyser. The geyser is dozens of meters high when the cavern is very compressible and the wellbore is narrow – at least at the brine outlet.

2. Brine outflow test

In salt caverns, a brine outflow test consists in measuring the flow rate of brine expelled from the cavern when the wellhead is opened, and the cavern and the wellbore are filled with saturated brine (Fig. 1). Examples are reported in various works [1–4]. This outflow results from two main phenomena: cavern creep closure, and thermal expansion (or contraction) of cavern brine.

2.1. Cavern creep closure

Creep closure originates in the gap between the geostatic pressure ($P_\infty = \rho_R g H$, where H is the cavern depth, $\rho_R = 2200$ kg/m^3 is rock density, and g is the gravity acceleration) and the cavern pressure ($P_c = \rho_b g H$, where $\rho_b = 1200$ kg/m^3 is the brine density). The creep closure rate can be noted as $\dot{\varepsilon}_{cr} V > 0$; it is a highly non-linear function of depth: $\dot{\varepsilon}_{cr} = 10^{-5}$/yr when $H = 250$ m and $\dot{\varepsilon}_{cr} = 3 \times 10^{-4}$/yr when $H = 1000$ m are typical.

2.2. Thermal expansion

Brine thermal expansion (or contraction) results from cavern brine warming (or cooling). Most often, caverns are leached out using water from a lake or a shallow aquifer; this water is colder than the rock temperature at the cavern's depth; when leaching is completed, cavern brine is still colder than the rock mass. Warming takes place, and the temperature gap decreases until it vanishes completely. It is a slow process, still slower when cavern is larger [5]. Let $t_{1/4}$ be the time

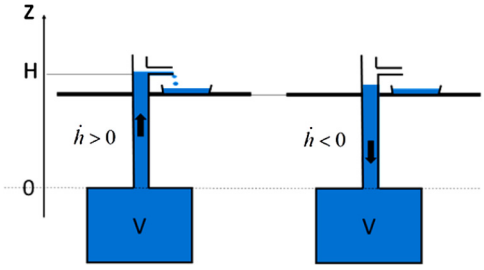

Fig. 1. Brine outflow test.

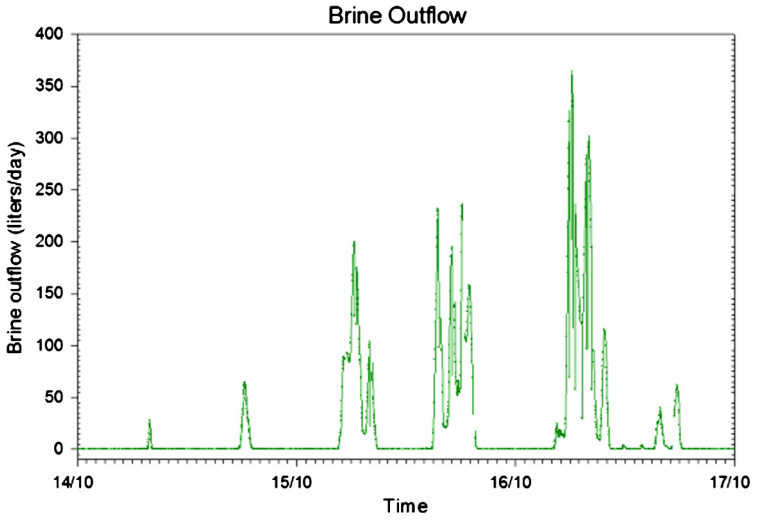

Fig. 2. Brine outflow rate between 14 October and 17 October 2008.

after which the initial temperature gap is divided by 4. In an idealized spherical cavern, $t_{1/4} = V^{2/3}/4k_{\text{salt}}$, where V is the cavern's volume and $k_{\text{salt}} = 100\ \text{m}^2/\text{yr}$ is the thermal diffusivity of salt – for instance, $V = 340\,000\ \text{m}^3$ and $t_{1/4} = 12$ yr. Brine warming results in brine expansion, as the brine equation of state can be written as $\dot{\rho}_\text{b} = \rho_\text{b}(\beta_\text{b}\dot{P} - \alpha_\text{b}\dot{T})$, where $\alpha_\text{b} = 4.4 \times 10^{-4}/°\text{C}$ is the thermal expansion coefficient of brine, and $\beta_\text{b} = 2.7 \times 10^{-4}/\text{MPa}$ is the compressibility coefficient of brine.

2.3. Brine outflow rate

A simple analysis suggests that the brine outflow rate is the sum of brine volumetric expansion and cavern closure rate:

$$S\dot{h} = \dot{\varepsilon}_\text{cr} V + \alpha_\text{b}\dot{T}_\text{c} V \tag{1}$$

where S is the wellbore cross-sectional area, and $\dot{h}$ is the brine rate in the wellbore. It could be expected that changes in the outflow rate are slow, as the two mechanisms responsible for brine expulsion are smooth. In fact, especially when the outflow is small (i.e. when the cavern is small, shallow, and old), it experiences abrupt changes that must be explained.

An example of this is a brine outflow test performed in the SG4-5 cavern operated by the "Compagnie des salins du Midi" at Gellenoncourt, France. This cavern is $H = 250$ m in depth and its volume is $V = 240\,000\ \text{m}^3$. The cavern had been kept idle for 30 years before the test, and thermal equilibrium was almost reached. Brine was collected at the ground level and weighed every two minutes [4]. It can be concluded from Fig. 2 that the brine flow rate often vanishes and that no-flow phases are followed by brine spews that last for a couple of hours. Atmospheric pressure changes must be considered.

3. Atmospheric pressure

More precise conditions are written than are used in Eq. (1). The mass conservation and equilibrium condition can be written as:

$$\rho_\text{b}[H,t] S\dot{h} = -\frac{\text{d}}{\text{d}t}\big(\rho_\text{b}[0,t]V\big) - \frac{\text{d}}{\text{d}t}\int_0^H \rho_\text{b}[z,t]S\,\text{d}z \tag{2}$$

$$P_\text{c} = P_\text{atm} + \int_0^H \rho_\text{b}[z,t]g\,\text{d}z \tag{3}$$

where P_atm is the atmospheric pressure; $z = 0$ at the cavern roof, and $z = H$ at the ground level (Fig. 1). The brine density $\rho_b[z < 0, t]$ is uniform in the cavern – brine is stirred by thermal convection. The mass changes in the wellbore (the integral in Eq. (2)) will be neglected (the wellbore volume is exceedingly small when compared to the cavern volume).

In this section, the changes in the atmospheric pressure are considered. A cavern pressure increase generates brine contraction and cavern expansion. An atmospheric pressure increase generates stress changes in the rock mass and contraction of the cavern. The mass conservation of changes in the cavern brine mass can be written as:

$$\frac{\text{d}}{\text{d}t}\big(\rho_\text{b}[0,t]V\big) = \rho_\text{b}(\beta_\text{b}\dot{P}_\text{c} - \alpha_\text{b}\dot{T}_\text{c})V - \rho_\text{b}V(\dot{\varepsilon}_\text{cr} - \beta_\text{c}\dot{P}_\text{c} + \beta_\infty\dot{P}_\text{atm}) \tag{4}$$

The coefficient of compressibility of the "hole" (β_c) reflects the elasticity of the rock mass; it depends on the elastic properties of the rock mass and the shape of the cavern, $\beta_c = \beta_c(E, \nu, \partial\Omega)$. In an idealized spherical cavern, $\beta_c = 3(1+\nu)/2E$; in an actual cavern, $\beta_c = 1.3 \times 10^{-4}$/MPa is typical. However, larger values are met sometimes – for example, when the cavern is somewhat flat [6] or when the cavern contains gas pockets, as discussed in Section 6. It is convenient to set $\beta = \beta_c + \beta_b$, as β is a quantity that is easy to measure in an actual cavern by shutting in the cavern, injecting some brine, and measuring the resulting pressure increase [6].

The effect of atmospheric pressure changes, which are transmitted through the rock mass (rather than through the brine-filled wellbore) is characterized by $\beta_\infty = \beta_\infty(E, \nu, \partial\Omega)$. When atmospheric pressure changes by $\dot{P}_{atm}$, the state of stresses in the rock mass changes accordingly. The dimensions of the horizontal domain, at the ground level, in which atmospheric pressure changes are almost uniform, is much larger than the cavern depth: in the rock mass underneath this domain, stress changes, $\underline{\underline{\dot{\sigma}}}^{\infty}$ are uniform and can be considered as "*oedometric*" – i.e. $\dot{\sigma}_{zz}^{\infty} = -\dot{P}_{atm}$, and $\dot{\sigma}_{xx}^{\infty} = \dot{\sigma}_{yy}^{\infty} = -\nu\dot{P}_{atm}/(1-\nu)$. These stresses generate cavern shrinkage (when $\dot{P}_{atm} > 0$) by $\dot{V} = -\beta_\infty V \dot{P}_{atm}$. In an idealized spherical cavern, $\beta_\infty = 3(1+\nu)/2E$. During the Gellenoncourt test described above, it was observed that $\beta_\infty/\beta = 0.54$.

In this section, brine density changes in the wellbore are neglected, and $\dot{P}_c = \dot{P}_{atm}$: atmospheric pressure changes are transmitted to the cavern both through the rock mass and through the wellbore brine column. Equations (2) and (4) can be simplified as

$$S\dot{h}/V = -(\beta - \beta_\infty)\dot{P}_{atm} + \alpha_b \dot{T}_c + \dot{\varepsilon}_{cr} \quad \text{when } \dot{h} > 0 \tag{5}$$

Note that this formula holds when $\dot{h} > 0$. When the brine/air interface drops in the wellbore (Fig. 1, right), $\dot{h} < 0$, $\dot{P}_c = \dot{P}_{atm} + \rho_b g \dot{h}$, and

$$(S + \rho_b g \beta V)\dot{h}/V = -(\beta - \beta_\infty)\dot{P}_{atm} + \alpha_b \dot{T}_c + \dot{\varepsilon}_{cr} \quad \text{when } \dot{h} < 0 \tag{6}$$

In the case of the Gellenoncourt cavern, the rate of creep closure was slow, $\dot{\varepsilon}_{cr} = 3 \times 10^{-9}$/day, $\beta - \beta_\infty = 2.5 \times 10^{-4}$/MPa, and an atmospheric pressure increase of a few hPa was able to interrupt the brine outflow (Fig. 2).

4. Brine temperature changes in the borehole

It was assumed in the previous section that $\dot{P}_c = \dot{P}_{atm}$: at any depth, brine density in the wellbore remained constant during brine outflow. In fact, temperature changes must be considered in Eq. (3). In the following, it is assumed that the cavern brine temperature (T_c) has reached equilibrium with the rock mass. In the rock mass, the geothermal temperature is an increasing function of depth, with $T_\infty(z) = T_c - \Gamma z$ ($\Gamma = 3 \times 10^{-2}$/m being typical). It was also assumed in previous sections that heat exchanges between the rock mass and the wellbore were so fast that thermal equilibrium was reached immediately: $T(z,t) = T_\infty(z)$. However, this assumption is incorrect, especially when the brine rate in the wellbore is fast enough, as explained below. It is assumed that at $t = 0$, brine begins rising in the wellbore with a constant rate of $\dot{h} = h/t$. A simple model consists in assuming that, at a given depth, the heat flux between the rock mass and the wellbore is proportional to the difference between the geothermal temperature and the brine temperature:

$$\frac{dT(z,t)}{dt} = \frac{\partial T(z,t)}{\partial t} + \dot{h}\frac{\partial T(z,t)}{\partial z} = -\frac{T(z,t) - T_\infty(z,t)}{t_c}; \quad T(z,0) = T_\infty(z); T(0,t) = T_c \tag{7}$$

When a is the wellbore radius, t_c is a characteristic time, $t_c = a^2/k_{salt}$ equals 1–2 hours, a value confirmed by experience. The solution to this partial derivative equation can be written:

$$\begin{cases} T(z,t) = T_c - \Gamma z + \Gamma \dot{h} t_c \left[1 - \exp(-t/t_c)\right] & \text{when } z - \dot{h}t > 0 \\ T(z,t) = T_c - \Gamma z + \Gamma \dot{h} t_c \left[1 - \exp(-z/\dot{h}t_c)\right] & \text{when } z - \dot{h}t < 0 \end{cases} \tag{8}$$

Heat exchange is fast when the brine rate is slow: $\dot{h}t_c \ll H$, and $T(z,t) \simeq T_\infty(z)$. It is slow (the behavior of brine in the wellbore is adiabatic) when $\dot{h}t_c \gg H$. For example, $H = 300$ m, $t_c = 1$ h, $S = 10^{-2}$ m^2, and the flow rate is adiabatic when it is significantly faster than $SH/t_c = 3$ m^3/h.

The derivative of the equilibrium equation ($\partial P/\partial z = \rho_b g$) with respect to time can be written as:

$$\frac{\partial^2 P(z,t)}{\partial z \partial t} = \rho_b g \left[-\alpha_b \frac{\partial T(z,t)}{\partial t} + \beta_b \frac{\partial P(z,t)}{\partial t}\right] \tag{9}$$

Equation (9) can be integrated with respect to z in the following form:

$$e^{-\rho_b g \beta_b H}\dot{P}_{atm}(t) - \dot{P}_c(t) = \alpha_b \rho_b g \Gamma \dot{h} \exp(-t/t_c)\frac{1 - e^{-\rho_b \beta_b g H}}{\rho_b g \beta_b} \tag{10}$$

Brine movement is so swift that atmospheric pressure can be considered as constant, $\dot{P}_{atm}(t) = 0$: the right-hand side of Eq. (10) is maximum when $t = 0, h = 0$ and $\dot{P}_c(t) \approx -\rho_b \alpha_b g \Gamma \dot{h} H$. From Eqs. (5) and (10), it can be inferred (only creep

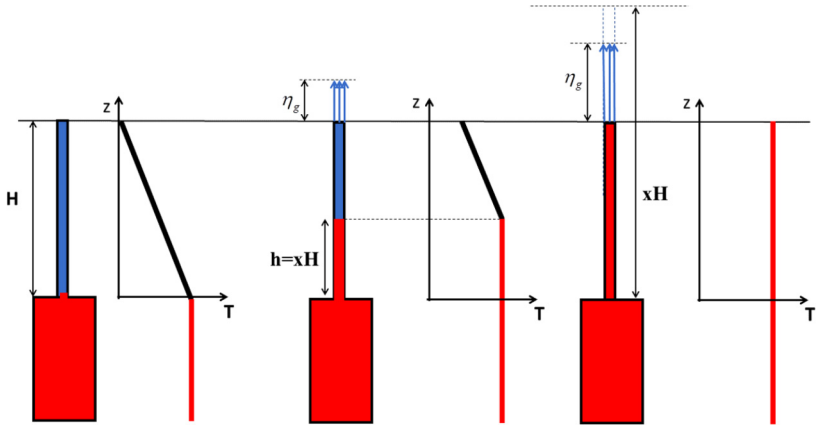

Fig. 3. Temperature distribution in the wellbore during and after the onset of a blowout.

closure is taken into account) that $\dot{h}(1-\beta V\rho_b g\alpha_b \Gamma H/S)=\dot{\varepsilon}_{cr}V/S$, and flow rate $S\dot{h}$ can be accelerated considerably by thermal effects when $(1-\beta V\rho_b g\alpha_b \Gamma H/S)$ is much smaller than 1. In such a case, $\dot{h}$ increases rapidly, and inertia terms and head losses must be considered, as discussed in the next section.

5. Geyser

In this section, the onset of a brine geyser is discussed. Because the creep-closure rate and the atmospheric pressure rate are slow, these two phenomena can be neglected; the brine behavior in the borehole will be considered as adiabatic and, when flowing upward in the borehole, brine experiences only minute temperature changes. Warm brine enters the wellbore through the casing shoe. The cavern brine pressure decreases. At the same time, cold brine is expelled from the wellhead. The average temperature of the brine column increases. Its weight decreases accordingly, leading to still faster brine outflow – at least when the cavern pressure drop is not too fast, i.e. when the cavern is very compressible – and inertia terms must be considered together with head losses in the wellbore.

5.1. Newton's equation of motion

The onset of the geyser is at $t=0$. Let $Sh(t)$ be the volume of brine expelled from the cavern after $t=0$. When $h<H$, h is the height of the warm brine/cold brine interface in the wellbore (Fig. 3). Brine outflow results in a cavern-pressure drop of $-Sh/\beta V$. The weight of the brine column, which was $\rho_b gSH$ before the geyser starts, decreases by $-\rho_b gS\alpha_b\Gamma(2Hh-h^2)/2H$ as long as $h>H$; when $h>H$, this weight has decreased by $(-\rho_b gS\alpha_b\Gamma H/2)$ and remains constant. At the wellhead, the brine pressure equals the atmospheric pressure. Newton's first law of motion applies to the brine column in the wellbore. Its mass is $\mu=\rho_b HS[1-\alpha_b\Gamma(2Hh-h^2)/2]\approx\rho_b HS$, and its acceleration is $\ddot{h}$. It is pushed upward by the changes in the brine column weight, but it is slowed by the cavern pressure decrease. Head losses also must be considered. As the flow becomes turbulent rapidly, it is assumed that they are proportional to the square of the outflow rate:

$$\rho_b SH\ddot{h}=-\frac{S^2}{\beta V}h+\rho_b g\alpha_b\Gamma\left(\frac{2Hh-h^2}{2}\right)S-F(S)\dot{h}^2;\quad 0<h<H,\ \dot{h}>0 \tag{11}$$

This equation holds until $\dot{h}=0$ or until $h=H$. In some cases, the geyser is so intense that, after some time, warm brine fills the wellbore ($h>H$), and Eq. (11) must be rewritten as:

$$\rho_b SH\ddot{h}=-\frac{S^2}{\beta V}h+\rho_b g\alpha_b\Gamma\frac{H}{2}S-F(S)\dot{h}^2;\quad h>H,\ \dot{h}>0 \tag{12}$$

To discuss these equations, it is convenient to set $x=h/H, \omega^2=S/\rho_b\beta VH$, $\gamma^2=g\alpha_b\Gamma/2$, and $f=F(S)/\rho_b SH$; then, the momentum equations can be rewritten:

$$\ddot{x}+\omega^2x-\gamma^2(2x-x^2)+f\dot{x}^2=0\quad 0<x<1,\ \dot{x}>0 \tag{13}$$

$$\ddot{x}+\omega^2x-\gamma^2+f\dot{x}^2=0\quad x>1,\ \dot{x}>0 \tag{14}$$

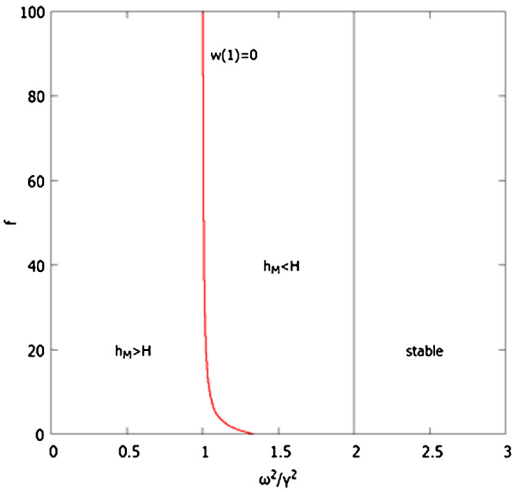

Fig. 4. The domain such that the interface remains in the borehole ($h_M = x_M/H < H$).

5.2. Integration of the momentum equation

Consider, first, Eq. (13) – the cold brine/warm brine interface is in the borehole ($x = h/H < 1$). This equation can be integrated with respect to time: $\dot{x}^2/2 + w(x) = e^{-2fx}\dot{x}_0^2/2$, where $\dot{x}_0 = \dot{x}(0)$ and

$$w(x) = \frac{\gamma^2}{2f}x^2 + \frac{\omega^2 - 2\gamma^2 - \gamma^2/f}{2f}\left(x - \frac{1}{2f} + \frac{e^{-2fx}}{2f}\right) \tag{15}$$

This equation is valid as long as $\dot{x} > 0$ and $x < 1$. It is assumed that $\dot{x}_0^2$ is exceedingly small; $w(x)$ is somewhat similar to a "potential" in a conservative mechanical system. The equilibrium position $x = 0$ is unstable when $w''(0) < 0$ – i.e. when $\omega^2/\gamma^2 < 2$. In such a case, the second derivative, $w''(x) = \gamma^2/f + (\omega^2 - 2\gamma^2 - \gamma^2/f)e^{-2fx}$, is monotonous, such that $w''(0) = \omega^2 - 2\gamma^2 < 0$, and $w''(\infty) > 0$; in the $]0, \infty[$ domain, it vanishes to zero once, when $x_i = \ln[1 + f(2 - \omega^2/\gamma^2)]/2f$, and x_i belongs to the $]0, 1]$ domain. The first derivative, $w'(x) = \gamma^2 x/f + (\omega^2 - 2\gamma^2 - \gamma^2/f)(1 - e^{-2fx})/2f$, is negative for small values of x (as $\omega^2 - 2\gamma^2 < 0$) and positive for high values of x. It can vanish only once in the $]x_i, \infty]$ domain, when $x = x_g$, $w'(x_g) = 0$. As $w(0) = 0$ and $w(\infty) = \infty$, $w(x)$ also vanishes once in the $]x_g, \infty]$ domain when $x = x_M$, $w(x_M) = 0$. As Eq. (14) holds only when $x = h/H < 1$, the zero of $w(x)$, or $w(x_M) = 0$, must be compared to 1. The curve $w(1) = 0$ cuts the $(\omega^2/\gamma^2, f)$-plane in two domains (see Fig. 4). Equation (15) holds in the sub-domain $h_M = Hx_M \leq H$.

When $x_M > 1$, Eq. (14) must be considered in the $]1, x_M]$ domain. It can be integrated with respect to time. When $x = 1$, the brine rate must be continuous; the solution can be written as $\dot{x}^2/2 + \bar{w}(x) = \dot{x}_0^2 e^{-f(x-1)/2}$, $w(1) = \bar{w}(1)$, and

$$\bar{w}(x) = \frac{\omega^2 x}{2f} - \frac{\gamma^2}{2f} - \frac{\omega^2}{4f^2} + \frac{\gamma^2}{4f^3}e^{2f(1-x)} + \frac{\omega^2 - 2\gamma^2 - \gamma^2/f}{4f^2}e^{-2fx} \tag{16}$$

The maximum value of x is reached when $\bar{w}(x_M) = 0$ (as $\bar{w}(1) < 0$ and $\bar{w}(+\infty) = +\infty$ – hence, $x_M > 1$). After this maximum is reached, the air/brine interface drops into the wellbore; after some oscillations, the system becomes quiet again.

The two cases ($x_M < 1$ and $x_M > 1$) are represented in Fig. 5 in the special case when $f = 0$ and $\omega^2/\gamma^2 = 2/3$ or $4/3$, and in Fig. 6 for several values of f when $\omega^2/\gamma^2 = 2/3$. Note that x_M such that $w(x_M) = 0$ does not depend much on the value of f, as expected from Eq. (16).

5.3. The no-head-loss case

When head loss is neglected, $f = 0$, the momentum equations [Eqs. (13) and (14)] can be integrated with respect to time:

$$\frac{\dot{x}^2}{2} + w(x) = \frac{\dot{x}_0^2}{2} \qquad w(x) = \frac{\omega^2 - 2\gamma^2}{2}x^2 + \gamma^2\frac{x^3}{3} \quad \dot{x} > 0,\ 0 < x < 1 \tag{17}$$

$$\frac{\dot{x}^2}{2} + \bar{w}(x) = \frac{\dot{x}_0^2}{2} \qquad \bar{w}(x) = \frac{\omega^2}{2}x^2 - \gamma^2 x + \frac{\gamma^2}{3} \quad \dot{x} > 0,\ x > 1 \tag{18}$$

Here again, two cases must be distinguished:

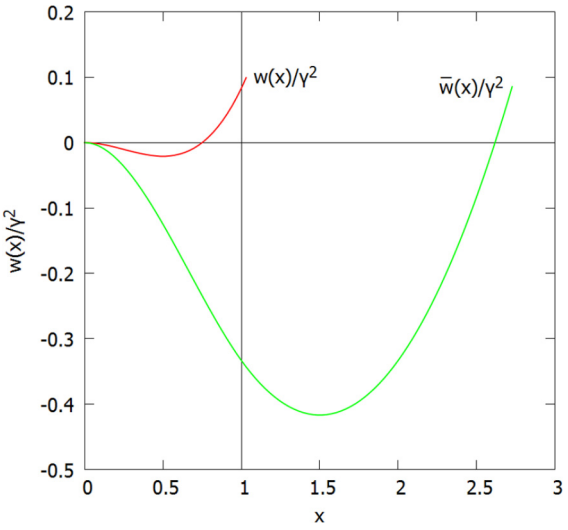

Fig. 5. "Potential" energy as a function of $x = h/H$; $f = 0$, $\omega^2/\gamma^2 = 2/3$ or $4/3$.

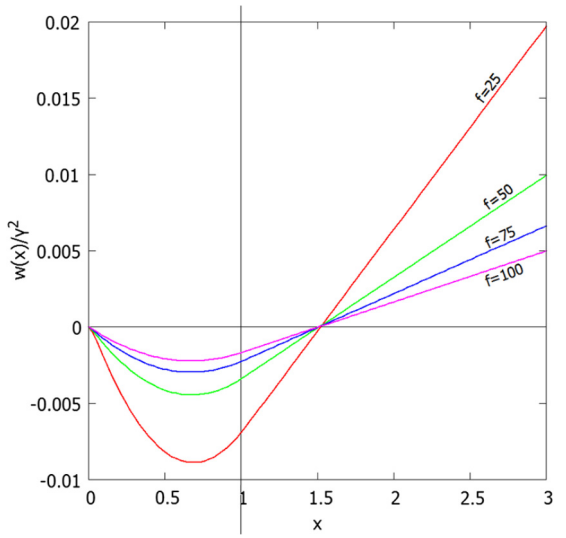

Fig. 6. "Potential" energy as a function of $x = h/H$ when $\omega^2/\gamma^2 = 2/3$, $f = 25$, 50, 75, and 100.

(1) when $2 > \omega^2/\gamma^2 > 4/3$, then $w(x)$ (and $\dot{x}$) vanishes to zero when $3(1 - \omega^2/2\gamma^2) = x_M < 1$. The warm/cold interface does not reach the wellhead. A maximum of $\dot{x}^2/2$ is reached when $w'(x_g) = 0$ or $x_g = 2 - \omega^2/\gamma^2$;
(2) when $\omega^2/\gamma^2 < 4/3$, the above solution still holds as long as $x \leq 1$; however, the geyser is still active when $x = 1$, and $x_M > 1$ (the cold/warm interface reaches the wellhead), as $w(1) < 0$. When $x > 1$, the well is filled with warm brine, and Eq. (18) must be used: $\bar{w}(x)$ (and $\dot{x}$) vanishes to zero when $w(x_M) = \omega^2 x_M^2/2 - \gamma^2 x_M + \gamma^2/3 = 0$, and the maximum of $\dot{x}^2/2$ is reached when $w'(x_g) = 0$ or $x_g = \gamma^2/\omega^2$.

The different cases are represented in Fig. 7. When ω^2/γ^2 is small, the geyser (of height Hx_g) can be quite high. However, this case is unrealistic, as, from a practical point of view, it implies that the cross-sectional area of the borehole (S) is small, as $\omega^2 = S/\rho_b \beta V H$. Head losses must be considered.

5.4. Height of the geyser

In principle, the height of the geyser is given by $\eta(t) = \dot{x}^2(t)/2g$. The highest geyser is reached when the brine rate is maximum – i.e. when $w'(x_g) = 0$ or $\bar{w}'(x_g) = 0$. However, wellheads often are equipped with a choke that increases both head losses and brine rate when the brine reaches the ground level. In such a case, the geyser can be higher than predicted by Eqs. (15) and (16).

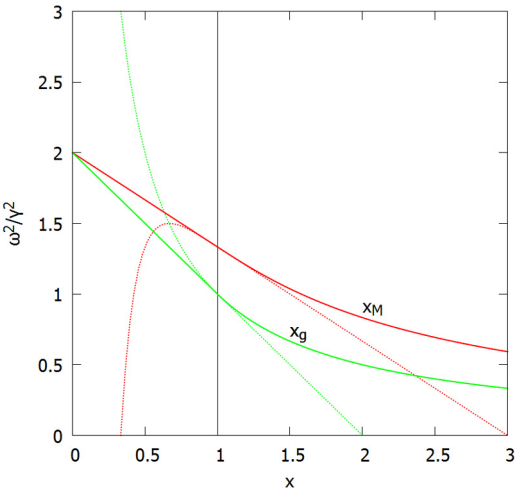

Fig. 7. x_M and x_g as a function of ω^2/γ^2 in the no head-loss case.

6. Discussion

It was proved that a geyser can appear when $w(0) = \omega^2 - 2\gamma^2 < 0$, or

$$\omega^2 = S/\rho_b \beta V H < \alpha_b \Gamma g = 2\gamma^2 \tag{19}$$

The right-hand side of this inequality does not depend on the characteristics of the cavern and does not vary much from one site to the other; $\alpha_b \Gamma g = 1.32 \times 10^{-4}$ s^{-2} is typical.

A geyser can appear in a large (V is large), deep (H is large) and compressible (β is large) cavern when the borehole cross-sectional area (S) is small enough. For instance, assuming $V = 400\,000$ m^3, $\beta = 5 \times 10^{-4}$/MPa and $H = 500$ m leads to $\rho_b \beta V H = 120$ m$^2 \cdot$ s^2, and the cross-sectional area must be smaller than $S < \alpha_b \Gamma g \rho_b \beta V H = 1.5 \times 10^{-2}$ m^2. Conversely, in the case of the Gellenoncourt cavern discussed above, $\beta V = 129.5$ m^3/MPa, $H = 250$ m, $S = 2.1 \times 10^{-2}$ m^2, $S/\beta V \rho_b H = 5.4 \times 10^{-4}$ s$^{-2} > g\alpha_b \Gamma$, and no geyser can appear.

Head losses are difficult to assess, as factors such as rugosity play a significant role. It often is accepted that head losses can be written: $\Delta P = \bar{f} \rho H V^2/2D$, where $\bar{f} = 0.015$ is typical in the turbulent domain. In this paper, head losses are defined as $\Delta P = F(S)\dot{h}^2/S$; hence, $f = F(S)/\rho_b S = \bar{f} H/2D$ and $f = 50$. Intensity of the geyser can be attenuated significantly by head losses, as proved by Fig. 6.

The conditions for the onset of a geyser are not often met, as a large cavern and a narrow wellbore are needed. However, several circumstances can be favorable. During an outflow test, crystallization often takes place in the wellbore (as the rock temperature at shallower depth is colder than the cavern-brine temperature), progressively leading to a smaller wellbore diameter. When leaching a salt cavern for brine production, air is often used as a "blanket": air is injected below the casing shoe to prevent any rise of the cavern roof. When leaching is completed, the cavern may contain pockets in which pressurized air remains trapped. In such a case, cavern compressibility increases drastically. For instance, when the cavern pressure is P_c, and ε is the fraction of the cavern volume that is occupied by gas, the cavern compressibility is $\beta + \varepsilon/P_c$; when $\varepsilon = 1\%$, $H = 500$ m, $P_c = 6$ MPa, $\varepsilon/P_c = 16 \times 10^{-4}$/MPa, and the cavern compressibility ($\beta = 4 \times 10^{-4}$/MPa when the cavern contains no gas) is multiplied by a factor of 5.

However, in such a case, the "thermal" geyser described in this paper – during which air remains trapped in pockets at the cavern roof – should not be confused with a blow-out resulting from a release of air from a trap, generated, for instance, by an atmospheric pressure drop, a phenomenon sometimes observed. An example of this may be provided by Fig. 8. In a brine cavern field in Switzerland [7], a dozen of caverns were at rest; they were left open, and the brine outflow was collected at the ground level. From one of these caverns, a 25-m-high geyser appeared unexpectedly and remained active over two and a half weeks. After some time, the geyser became intermittent. Air had been used as a blanket medium. Little information is available; whether this geyser is "tepid" or results from trapped air release rising in the wellbore is unclear at this time.

Acknowledgement

Special thanks are addressed to Kathy Sikora.

Fig. 8. A geyser above an underground cavern [7].

References

[1] B. Hugout, Mechanical behavior of salt cavities – in situ tests – model for calculating the cavity volume evolution, in: H.R. Hardy Jr., M. Langer (Eds.), The Mechanical Behavior of Salt, in: Proceedings of the Second Conference, Trans. Tech. Pub., Clausthal-Zellerfeld, Germany, 1988.

[2] P. Bérest, P.A. Blum, Mesure des déformations d'une caverne induites par les marées terrestres, C. R. Acad. Sci. Paris, Ser. IIb 316 (1993) 1341–1347 (in French).

[3] B. Brouard, On the Behavior of Solution-Mined Caverns, PhD Thesis, École polytechnique, Palaiseau, France, 27 January 1998 (in French).

[4] B. Brouard, P. Bérest, V. de Greef, J.-F. Béraud, C. Lheur, E. Hertz, Creep closure rate of a shallow salt cavern at Gellenoncourt, France, Int. J. Rock Mech. Min. Sci. 62 (2013) 42–50.

[5] M. Karimi-Jafari, P. Bérest, B. Brouard, Thermal effects in salt caverns, in: Proc. SMRI Spring Meeting, Basel, Switzerland, 2007, pp. 165–177.

[6] P. Bérest, J. Bergues, B. Brouard, Review of static and dynamic compressibility issues relating to deep underground salt caverns, Int. J. Rock Mech. Min. Sci. 36 (1999) 1031–1049.

[7] Schweizer Radio und Fernsehen, Play SRF, Messungen nach Salzwasserfontäne, https://www.srf.ch/play/tv/schweiz-aktuell/video/messungen-nach-salzwasserfontaene?id=801a0fa3-a341-409e-b53f-b0f51f90c577\&station=69e8ac16-4327-4af4-b873-fd5cd6e895a7, viewed 8 January 2018.